JOURNAL OF MATERIALS SCIENCE 29 (1994) 4975–4983

Improvement of sintering and piezoelectric properties of soft lead zirconate titanate ceramics

M. VILLEGAS, C. MOURE, J. R. JURADO, P. DURÁN
Instituto de Cerámica y Vidrio (CSIC), Electroceramics Department, 28500 Arganda del Rey, Madrid, Spain

Niobium-doped $Pb(Zr_{0.53}Ti_{0.47})O_3$ (PZTN) ceramics were prepared by the conventional (mixed oxides) method, modified by the addition of a PZT colloid of the same composition. The colloidal precursor was prepared using a coprecipitation method. Such an addition produced a significant improvement in the sinterability of a conventionally prepared PZTN powder and the sintering temperature was reduced, achieving a density $\geqslant 98\%$ theoretical density at 1075 °C for 2 h. The measured piezoelectric properties were as high as $k_p = 0.62$ and $d_{33} = 330 \times 10^{-12}$ C N^{-1}.

1. Introduction

Lead zirconate titanate (PZT) material continues to be a well-studied system because of its importance in piezoelectric applications. However, the measured properties of PZT materials synthesized by the conventional technique have been shown to be sensitive functions of the processing method, calcining temperature and sintering parameters [1–7]. In fact, a major problem in ceramic processing is to produce improved and reproducible ceramic materials having the required electromechanical properties. This lack of reproducibility in properties lies in the inability to control the specified microstructural development which, for sintered materials, depends on the characteristics of the starting powder [8], green compact microstructure [9] and sintering processes, because microstructures developed during sintering are essentially determined by powder characteristics and packing [10].

In PZT ceramics it is difficult to maintain material stoichiometry during thermal processing steps, such as calcining and sintering, because of volatility of lead (Pb) and lead oxide (PbO). Any deviation in composition caused by volatilization of these components adversely affects densification [11–13] and this results in a degradation of the piezoelectric properties. In this sense, it is known that sintering temperature can be reduced if the synthesis is made by a "wet" technique so that spatial compositional fluctuations are avoided [14] and particle size is kept small [15]. Another method to reduce the sintering temperature is doping ceramics with low-melting oxides, but previous research [16–19] has shown that microstructure and properties of the piezoelectric ceramics obtained at such low sintering temperatures are degraded. One of the reasons for the lowering of the piezoelectric properties is the excess of low-melting oxides as the non-ferroelectric phase is precipitated in grain boundaries [20–21].

The objective of our investigation was to reduce the sintering temperature of conventionally prepared PZTN powders without degrading their piezoelectric properties through the use of PZTN colloidal additions of the same composition as the conventional matrix and to obtain dense and uniform microstructures with the same piezoelectric phase surrounding conventional PZTN grains.

2. Experimental procedure

2.1. Colloid preparation

Two types of colloidal powders of the same composition $[Pb(Zr_{0.53}Ti_{0.455}Nb_{0.015})O_3]$ were prepared by a coprecipitation technique using two different alcohols as mixing and washing media: ethanol or isopropanol (denoted ET and IS powders, respectively).

The starting raw materials were PbO (Merck 7041), Nb_2O_5 (Fluka 7252) and zirconium and titanium tetrabutoxides (Ventron 88718 and Ventron 77124, respectively). The characteristics of the oxides employed are summarized in Table I.

A solution of the butoxides in ethanol or isopropanol was added while stirring to a suspension which contained the lead and niobium oxides in a 6 N NH_4OH aqueous solution. This addition produces simultaneous hydrolysis of the raw materials and the consequent formation of the coprecipitated powder. After coprecipitation this powder was washed with a solution [alcohol/H_2O] 75/25 to eliminate the residual ammonia. The dry powder ($\sim$ 35 °C for 24 h when using ethanol and $\sim$ 70 °C when using isopropanol) was milled for 4 h in a planetary mill with ZrO_2 balls and the corresponding alcohol. The preparation method is summarized in Fig. 1.

0022–2461

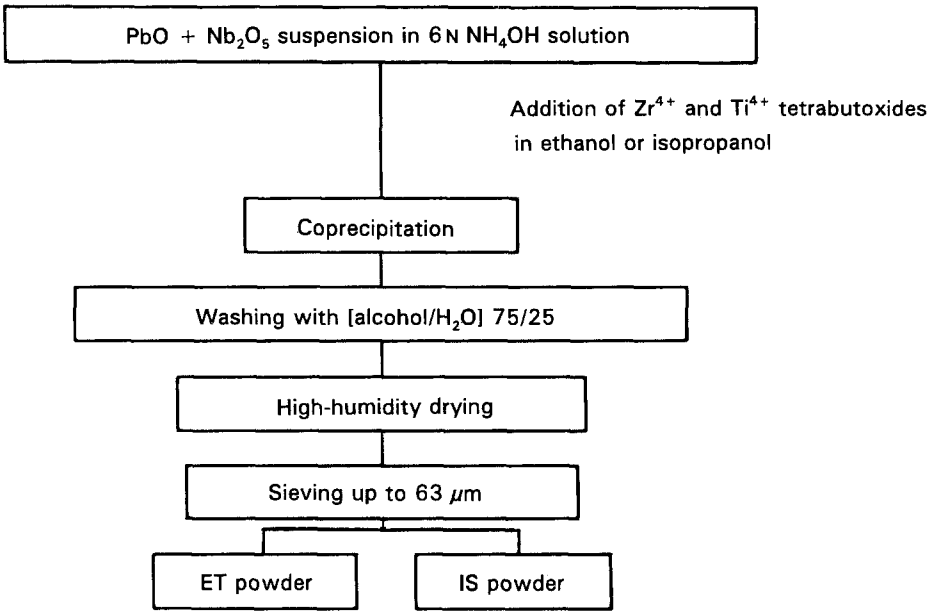

Figure 1 Flow diagram of the preparation of the colloidal PZTN.

TABLE I Physical characteristics of the different oxides employed during PZTN synthesis

Oxide	Structure	Purity (%)	Crystal size by XRD (nm)	Specific surface area by BET ($m^2 g^{-1}$)
PbO	Orthorhombic	99	430	0.06
Nb_2O_5	Monoclinic	99.9	90	3.8 ± 0.2
ZrO_2	Monoclinic	99.9	9	53 ± 3
TiO_2	Tetragonal	99	20	10.3 ± 0.5

2.2. Oxide powder synthesis

Reagent-grade commercial oxides (characteristics summarized in Table I), PbO, Nb_2O_5, ZrO_2 (Dinamit Nobel) and TiO_2 (Tioxide AH-R), were used to prepare PZTN powder with the same composition as colloidal powders reported in the previous section. A conventional technique including calcination at 850 °C for 4 h was employed. After attrition milling in isopropanol and calcining, the powder was dried in a revolving evaporator and sieved. The preparation method of this powder is shown in Fig. 2.

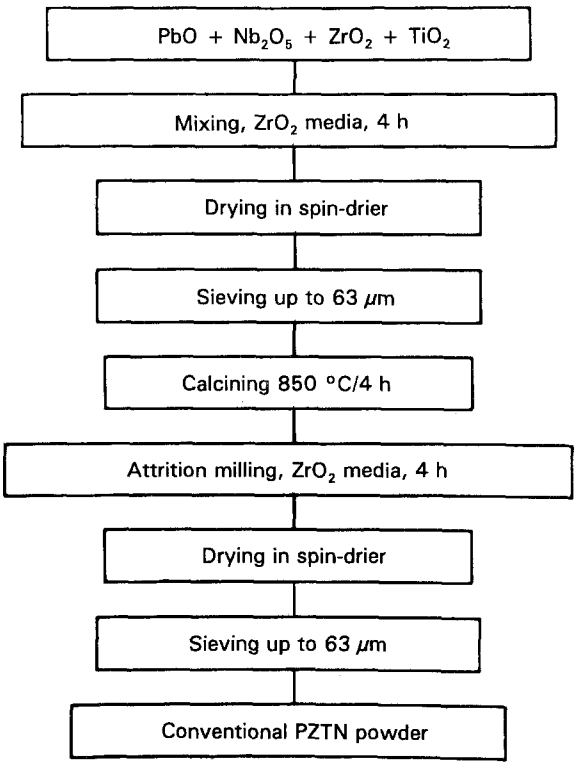

Figure 2 Flow diagram of the preparation of the conventional PZTN powder.

2.3. Powder characterization and sample preparation

The addition of colloidal powders to the PZTN oxide powder was made using a high shear mixing device to obtain a good mixing of the colloidal and oxide powders, and ethanol or isopropanol, as liquid media during the mixing process, were used. The amount of colloidal powder additions were 1 and 2 wt %. Lower and higher colloidal powder concentration led to poorer results, as reported elsewere [22].

The different powders obtained (coprecipitated, calcined PZTN and PZTN with colloidal additions) were characterized by means of X-Ray diffraction (XRD) (Siemens Diffraktometer D5000, Germany), sedigraphy (Micromeritics Sedigraph 5000 ET, USA), differential thermal and thermogravimetric analysis (ATD–TG) (Mettler TA-200, Switzerland), the single-point Brunauer–Emmet–Teller (BET) method (Quanta Chrome, USA) and scanning electron microscopy (SEM) (Zeiss DSM 950, Germany).

PZTN powder with colloidal additions was axial (37 MPa) and isopressed (200 MPa) into discs about 2 cm diameter and 0.5 cm thick. Sintering was performed in air without using a PbO buffer and the samples were placed on a platinum foil and covered with a high-purity Al_2O_3 crucible without sealing. On

sintered samples the apparent density was measured by the Archimedes method with water, and weight losses were determined by weighing the samples before and after sintering. The microstructure of the fired samples was studied by scanning electron microscopy on fresh fractured surfaces and the average grain size was measured by the line intercept method [23]. The piezoelectric properties were studied on selected discs electroded in both faces with silver paste and poled at 40 $kV\,cm^{-1}$ for half an hour in an oil bath at 120 °C. Piezoelectric measurements were carried out by IEEE standards using a Vectorial Impedance Analyser (4192 A Hewlett Packard, USA) and all calculations were made following the resonance method [24]. To measure d_{33} parameter, a Berlincourt Piezo-*d* meter (CADT, Channel Products, USA) was employed.

3. Results and discussion

3.1. Study of the conventional PZTN powder

After calcining, conventional PZTN powder was found to be a mixture of rhombohedral and tetragonal perovskite phases, by means of XRD. This result was due to compositional fluctuations that arise during conventional synthesis [25], taking into account that the PZTN composition was in the morphotropic phase boundary. Traces of PbO and ZrO_2 were also observed, indicating that PZTN formation was not complete. A small amount of $PbZrO_3$ was also present, showing that conventional synthesis proceeded with $PbZrO_3$ formation at intermediate stages as a consequence of the characteristics of the ZrO_2 powder used as raw material [26, 27] (see Table I). After attrition milling, the crystal size of the PZTN powder, as determined by XRD, was 34 nm, and its specific surface area, measured by BET, was about 1.5 $m^2\,g^{-1}$.

SEM study of this conventional PZTN powder, as shown in Fig. 3, revealed the presence of agglomerates in which the primary particle size had an average size of 35 μm, as measured by the line intercept method [23]. This exceptionally small size shows the high efficiency of attrition milling in reducing particle size. Agglomeration of this powder was relatively high with an average agglomerate size of 1.5 μm, but these agglomerates seemed to be soft and thus they could easily be broken during pressing.

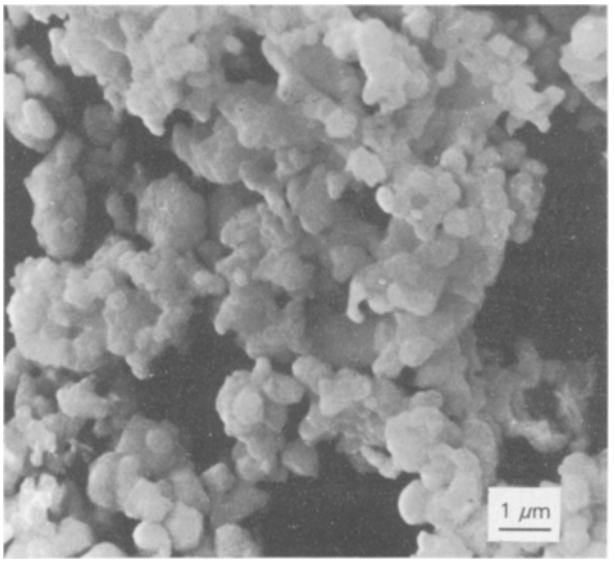

Figure 3 Scanning electron micrograph of conventional PZTN powder calcined at 850 °C for 4 h.

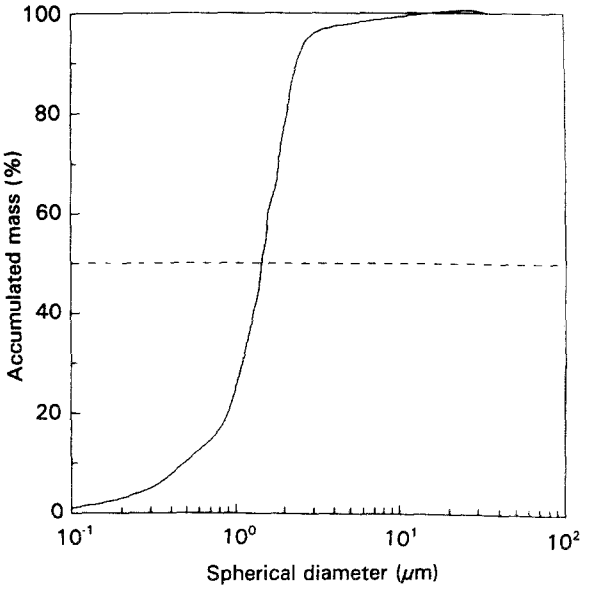

Figure 4 Sedigraph curve of conventional PZTN powder calcined at 850 °C for 4 h.

Fig. 4 shows that the average particle size of conventional PZTN powder, as measured by Sedigraphy, was about 1.6 μm and more than 90% of the particle size ranged from 0.1–2 μm. This fact would also facilitate the sintering of this powder [15]. The higher average particle size measured by Sedigraphy when compared with that observed by SEM (0.35 μm) reveals that such a technique gives the average agglomerate size rather than average particle size [28]. In this way, Sedigraph measurements are a good indication of powder agglomeration.

3.2. Study of the colloidal powders

XRD analysis of the colloidal powders obtained using both ethanol or isopropanol indicated that both were mainly amorphous, although small diffraction peaks corresponding to traces of free PbO were present. SEM study of these powders showed that in spite of the high shear mixing treatment and milling, both powders (ET and IS) were highly agglomerated (see Fig. 5). Particle size was not measured, because the SEM technique has insufficient resolution to distinguish the small particles of the coprecipitated powders. However, an estimation of the smallest agglomerate size could be done, this being 50 nm for both powders. It must be mentioned that the agglomeration stage of ET powder was somewhat higher than that of IS powder. The presence of a higher residual liquid content, which produces higher agglomeration, in ET powder when compared with IS, is due to the drying temperature employed (~ 35 °C) which is lower than that necessary to produce ethanol combustion (~ 78 °C). IS powder drying was done at

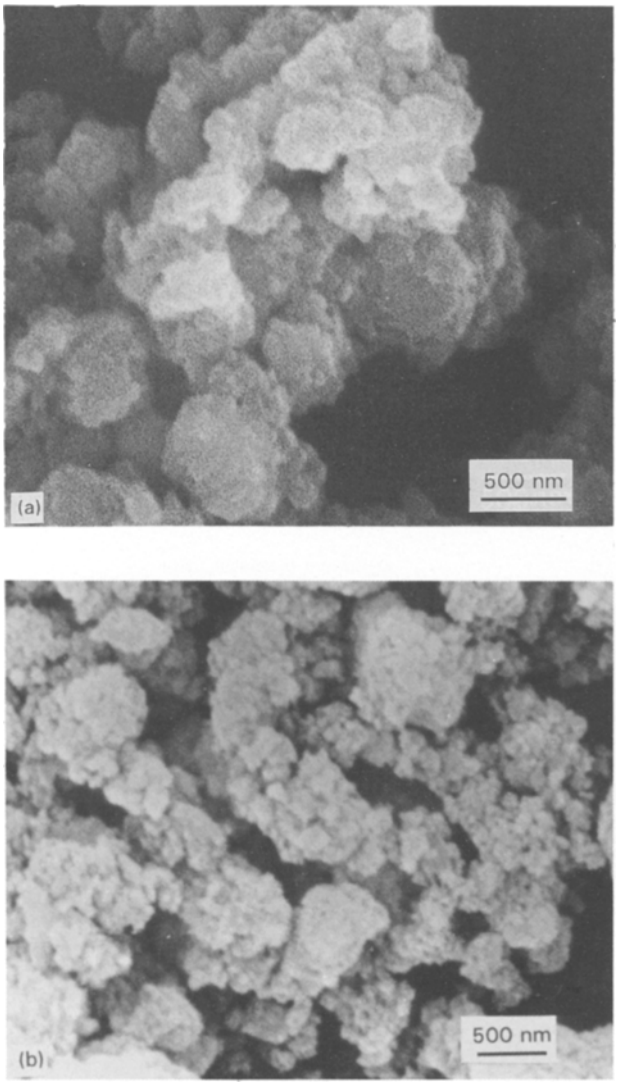

Figure 5 Scanning electron micrographs of (a) ET and (b) IS coprecipitated powders.

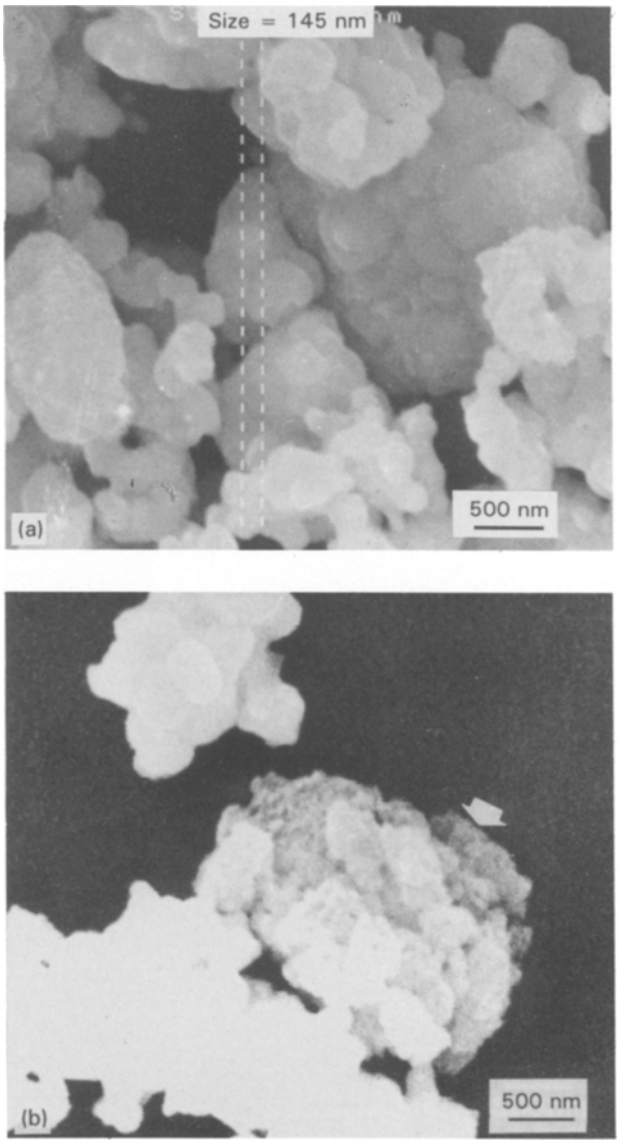

Figure 6 Scanning electron micrographs of (a) PZTN + x% ET and (b) PZTN + x% IS powders.

$\sim 70\,^{\circ}C$, a temperature nearer to that of isopropanol combustion ($\sim 82\,^{\circ}C$), so this powder contains less residual alcohol adsorbed on the particles.

3.3. Study of PZTN + x % colloid compositions

The results of the BET study of this powder showed that there was an appreciable change in the specific surface area between PZTN powder with and without colloidal additions (2.4 ± 0.1 and $1.40 \pm 0.07\ m^2\,g^{-1}$, respectively). The enhanced specific surface area could be due to the high value of this parameter in the colloidal powders ($\sim 100\ m^2\,g^{-1}$).

Scanning electron micrographs of PZTN + x% colloid powders (Fig. 6) showed that average particle size of conventional PZTN powder is again $\sim 0.35\ \mu m$, as in the powder without additions, so the high shear mixing treatment does not reduce the particle size and it only is useful to homogenize these powders. Fig. 6 also shows the agglomerated colloidal powder, which corroborates the above result.

A microstructural study by SEM on fresh fractured surfaces of the green compacted samples is shown in Fig. 7 and, can be seen, a very uniform compaction, which correlated well with the green density data listed in Table II, is observed. The high green density measured in samples containing colloidal additions was probably due to its lubricant effect, which allowed a better rearrangement of the powder particles during pressing. The main feature of this method is that colloidal powders were converted into fine PZTN particles by heat treatment at $\sim 500\,^{\circ}C$, as can be seen from DTA–TG studies (Fig. 8), and these fine particles fill the voids formed during pressing of PZTN powder, giving rise to a very green density ($\sim 63\%\ \rho_{th}$). Such a higher green density could lead to an enhancement of the sintering density.

TABLE II Green density of the prepared compositions

Sample	$\rho_g\ (g\,cm^{-3})$	$\rho_g\ (\%\,\rho_{th})$
PZTN + 1% ET	5.05 ± 0.06	63 ± 2
PZTN + 2% ET	5.13 ± 0.06	64 ± 2
PZTN + 1% IS	5.13 ± 0.06	64 ± 2
PZTN + 2% IS	5.05 ± 0.06	63 ± 2

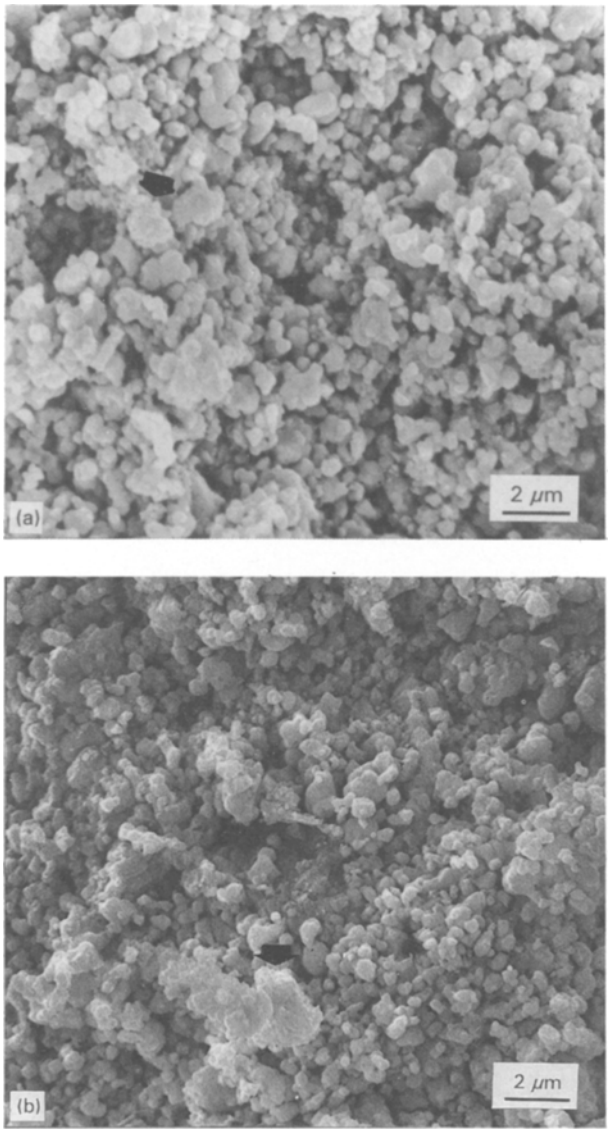

Figure 7 Scanning electron micrographs of fresh fracture surfaces of (a) PZTN + x% ET and (b) PZTN + x% IS green compacts.

3.4. Sintering

Studies of densification and weight losses were carried out as a function of sintering temperature and time in the range of 1000–1125 °C and 1–8 h, respectively. The maximum density obtained, as shown in Figs 9 and 10, was ⩾98% theoretical density at 1075 °C for 2 h. However, a sintering temperature range of 1050–1075 °C and a soaking time of 2–4 h in which the density remained almost constant could be established. These temperatures are almost 150–200 °C lower than those generally used during sintering of PZTN materials in the conventional method (> 1200 °C) [1–3], and also lower than those employed for the sintering of chemically prepared PZTN materials [4, 29]. These low sintering temperatures represent an important innovation in the processing of this kind of material given that no fluxes are used and, therefore, the piezoelectric properties of the PZTN ceramics so obtained would not be degraded.

Weight variation studies showed that all samples suffered weight losses of about 2%–3% during sintering and, as would be expected, they raised with sintering temperature. These low weight losses could

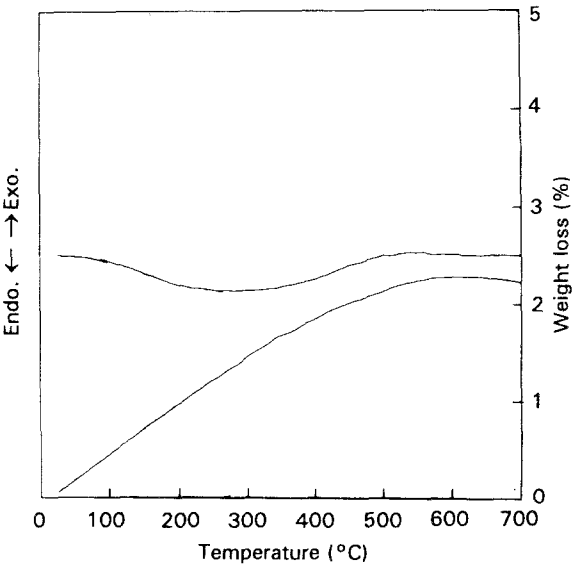

Figure 8 DTA–TG curves of PZTN + 1% ET composition.

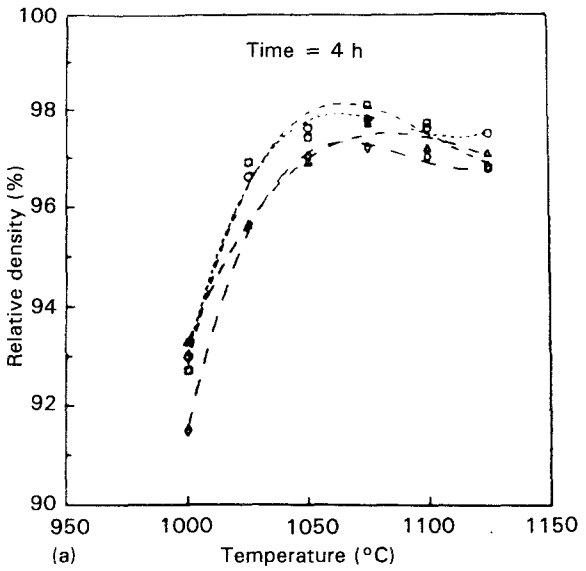

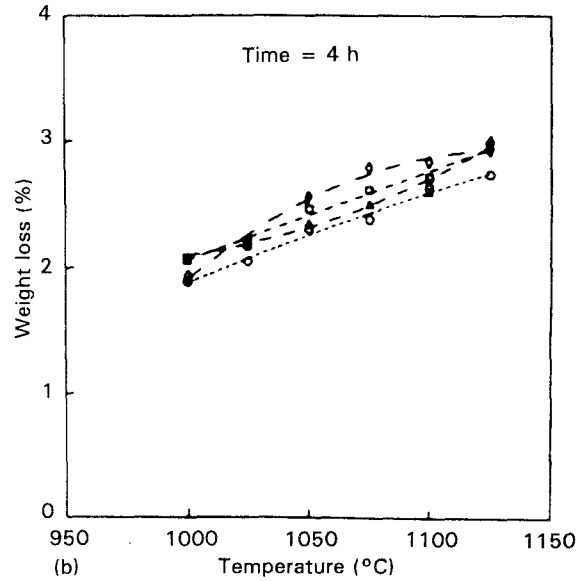

Figure 9 (a) Density and (b) weight loss curves as a function of temperature for the prepared compositions. (○) PZTN + 1% ET, (□) PZTN + 2% ET, (△) PZTN + 1% IS, (◇) PZTN + 2% IS.

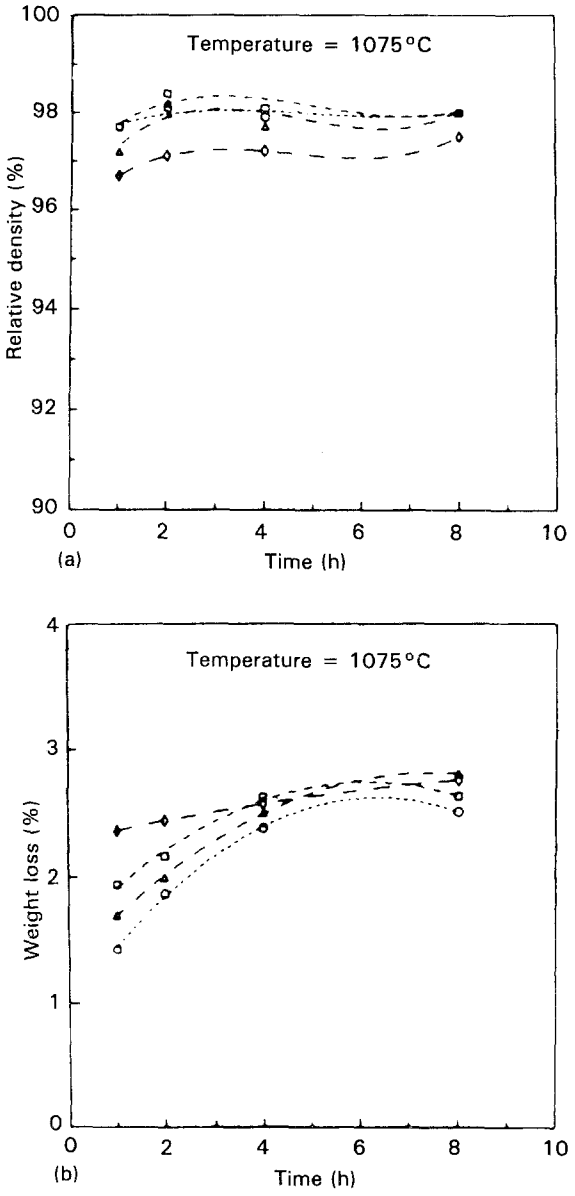

Figure 10 (a) Density and (b) weight loss curves as a function of time for the prepared compositions. For key, see Fig. 9.

be attributed to volatilization of decomposition products from the colloidal additions, see Fig. 8. So, PZTN ceramics obtained after sintering were mainly stoichiometric or slightly deficient in PbO, and this fact is very important given that sintering was performed without using a buffer. The reasons for these slight weight losses are the low sintering temperature, at which PbO activity is still small [30, 31], and also to the presence of colloidal powders, which could be acting as an internal buffer controlling the PbO losses from the PZTN conventional matrix.

Table III summarizes the main physical properties of the most representative sintered samples. It must be mentioned that, after sintering, all the samples had rhombohedral perovskite structure, indicating a very small compositional fluctuation.

3.5. Microstructure

Microstructure development can be seen in the fracture surfaces of samples and, as shown in Fig. 11, a bimodal grain-size distribution is observed. According

TABLE III Main physical properties of the best sintered samples

Sample	Sintering temp (°C)/ time (h)	% ρ_{th}	% weight loss
PZTN + 1% ET	1075/2	98.1 ± 0.6	1.9 ± 0.1
PZTN + 2% ET	1075/2	98.4 ± 0.6	2.2 ± 0.1
PZTN + 1% IS	1075/2	98.2 ± 0.6	2.0 ± 0.1
PZTN + 2% IS	1075/2	97.5 ± 0.6	2.8 ± 0.1

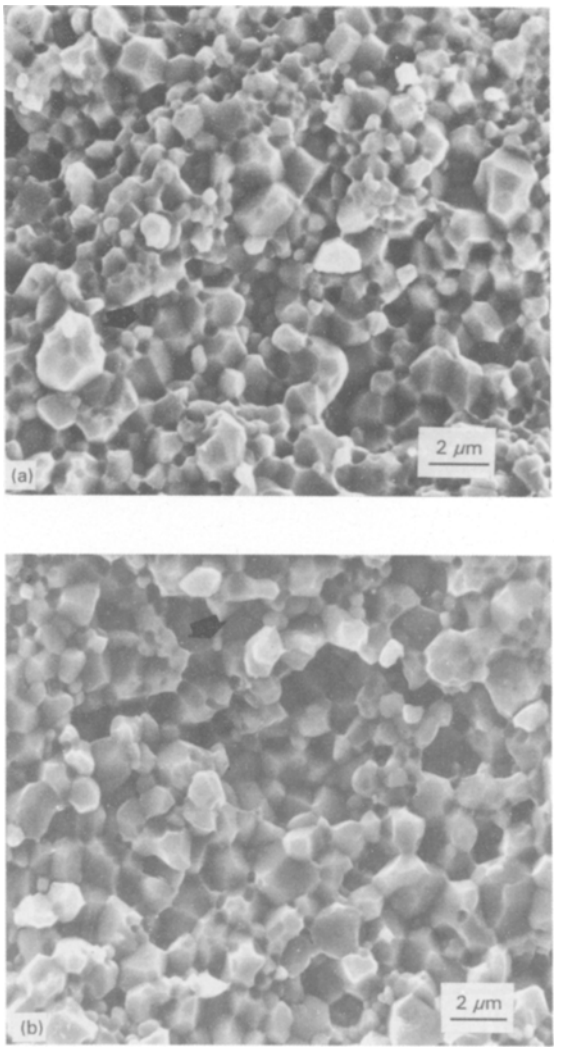

Figure 11 Scanning electron micrographs of fracture surface of (a) PZTN + 1% ET and (b) PZTN + 1% IS, sintered at 1075 °C for 2 h.

to the processing route employed, grains of about 2.0 μm from the conventional oxide powder surrounded by grains of about 0.5 μm from the colloidal one were developed. The fracture type is mainly considered to be intergranular and, in general, microstructure is quite homogeneous with very little porosity in which the grains from colloidal phase were located mainly in both the triple points and the grain boundaries. Such a grain distribution is consistent with the high density of the sintered materials, this being an unusual result for the conventional oxide processing route.

3.6. Piezoelectric properties

The piezoelectric properties measured on 98% dense

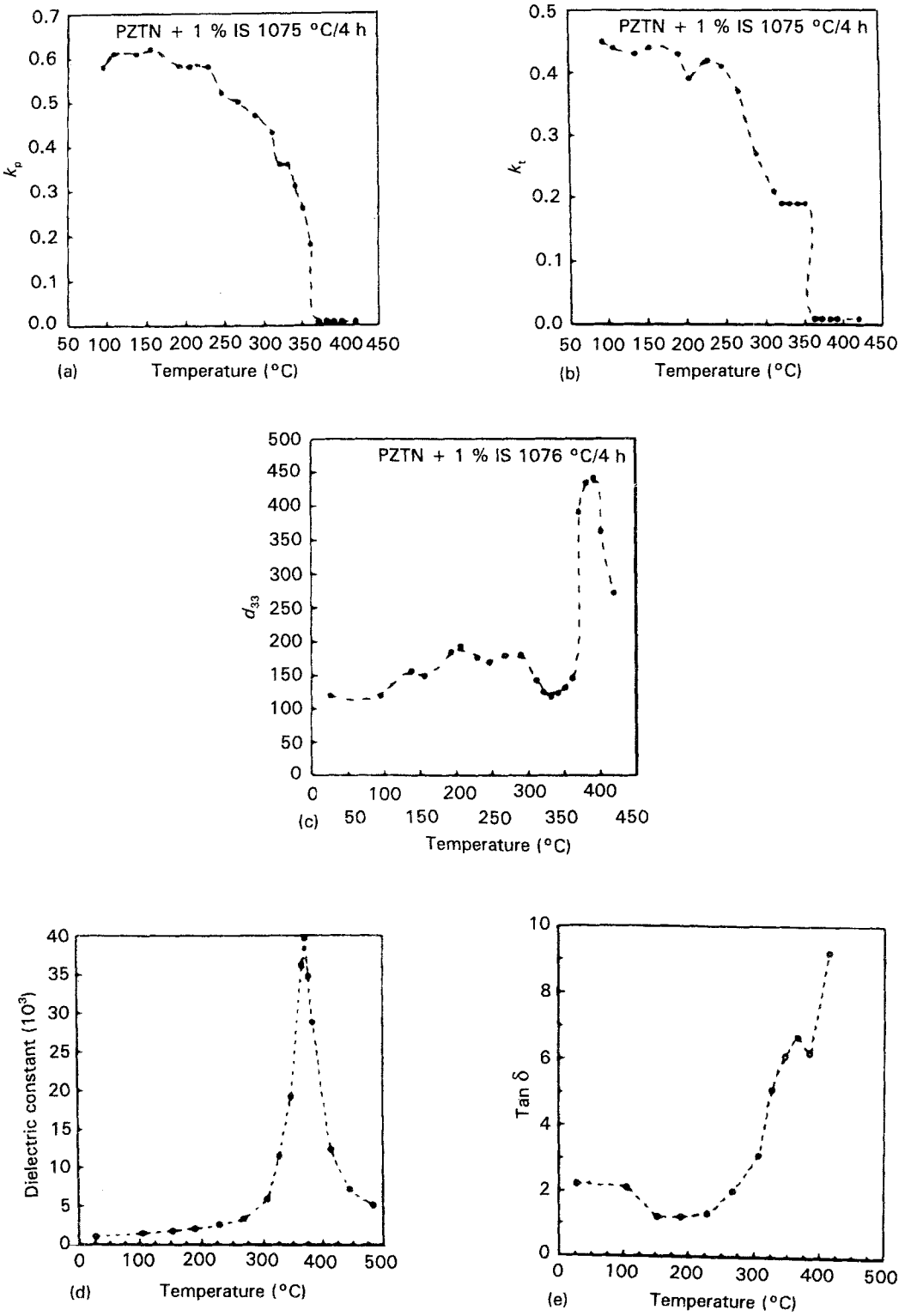

Figure 12 (a–e) Variation of the dielectric and piezoelectric properties as a function of temperature.

samples were higher than those currently achieved in conventional PZTN ceramics, as shown in Table IV. Thus a k_p as high as 0.6 and a d_{33} higher than 300 $\times 10^{-12}$ C N^{-1} could be measured. The high value of piezoelectric parameters measured in these materials could be closely related to their good stoichiometry, high density, and relatively small grain size [32, 33]. These results are in close agreement to those reported by Webster *et al.* [13] who found that better piezoelectric properties in rhombohedral PZT materials were obtained when they were stoichiometric or slightly PbO deficient, because, in this case, composition shifts towards the morphotropic phase boundary [34] and also because the creation of Pb^{2+} vacancies facilitates domain wall motion [35].

As is shown in Fig. 12, the influence of temperature on the piezoelectric properties was studied between room temperature and 450 °C. It can be seen that the piezoelectric parameters had an acceptable and almost constant value ($k_p \geqslant 0.50 \pm 0.01$ and $d_{33} \geqslant 300 \times 10^{-12}$ C N^{-1}) as the temperature increased up to ~ 250 °C. This fact indicates the high polarization stability of the materials containing colloidal additions. Only at temperatures as high as the Curie

TABLE IV Electromechanical properties of the most representative sintered samples

Sample	k_p	K_{3T}	Tan δ (%)	Q_m	d_{33} (10^{-12} C N^{-1})
PZTN + 1% ET 1075/2	0.58 ± 0.01	1037 ± 8	2.1	63	295 ± 10
PZTN + 2% ET 1075/2	0.62 ± 0.01	1063 ± 9	2.2	73	338 ± 14
PZTN + 1% IS 1075/2	0.61 ± 0.01	1076 ± 9	2.1	81	316 ± 12
PZTN + 2% IS 1075/8	0.61 ± 0.01	1061 ± 9	1.9	73	290 ± 10

TABLE V Comparison of the data obtained in this work with other data in the literature

K_3^T	k_p	Tan δ (%)	Ref.
1063 ± 9	0.62 ± 0.01	2.2	PZTN + 2% ET 1075/2
600 ± 4	0.54 ± 0.01	2.0	PZTN 1160/4
750	0.56	–	[13]
1450	0.53	–	[36]
1500	0.55	1.8	[37]
685	0.54	2.3	[38]
1100	0.54	0.4	[19]

temperature (380 ± 5 °C), as was expected, were the piezoelectric parameters strongly decreased, as a consequence of the ferroelectric–paraelectric phase transition where the material is depoled. In the d_{33} curve, abnormal behaviour was present. This could be explained by taking into account the expression used to calculate this piezoelectric parameter

$$d_{33} = k_{33}(\varepsilon' K_3^T s_{33}^E)^{1/2} \quad (1)$$

so the decrease in d_{33} is due to the drop of both the electromechanical coupling factor, k_{33}, and the elastic compliance, s_{33}^E, as the temperature increased up to 340 °C (see Fig. 12). Above that temperature, d_{33} was enhanced as a consequence of the strong dielectric constant increasing near the Curie temperature. This stability of piezoelectric parameters as a function of temperature is important for technical applications of these materials, for example, in the manufacture of high-frequency piezoelectric transducers in which temperatures around 80–100 °C are needed [20].

Table V compares the values of piezoelectric parameters obtained in this work with those of conventional PZTN powder without colloidal additions, and also with other values reported in the literature of PZTN conventional materials.

4. Conclusion

The addition of 1–2 wt % PZTN colloidal powders to PZTN calcined ones enhanced the density of the green compacts, and simultaneously reduced its sintering temperature by at least 150 °C. As a consequence, the PbO weight losses were better controlled and no compositional fluctuations were found in the highly (⩾98% theoretical density) densified bodies. Colloidal additions were found to be well distributed in the green microstructure and, as a consequence, an homogeneous microstructure was developed after sintering. Piezoelectric properties obtained in the samples modified by colloidal additions were better than those corresponding to the conventional PZTN ceramics, attaining k_p and d_{33} values higher than 0.6 and 300 $\times 10^{-12}$ C N^{-1}, respectively.

References

1. F. KULCSAR, *J. Am. Ceram. Soc.* **42** (1959) 343.
2. Y. S. KIM and R. J. HART, in "Materials Science Research", Vol. 11 (Pergamon Press, New York, 1987) pp. 323–33.
3. S. H. CHO and J. V. BIGGERS, *J. Am. Ceram. Soc.* **66** (1983) 743.
4. M. VILLEGAS, C. MOURE, J. R. JURADO and P. DURAN, *J. Mater. Sci.* **28** (1993) 3482.
5. S. S. CHANDRATREYA, M. R. FULRATH and J. A. PASK, *J. Am. Ceram. Soc.* **64** (1981) 422.
6. T. TSUZUKI, in "Proceedings of the 1st Meeting on Ferroelectric Materials and Their Applications", Kyoto Japan, November 1977, edited by M. Marutake, K. Shibayana, T. Ikeda and N. Ichinose (Keihin Pronting Co., Tokyo, Japan, 1978) pp. 175–80.
7. Y. YOSHOKAWA, T. TSUZUKI, T. KOBAYASHI and A. TAKAGI, *J. Mater. Sci.* **23** (1988) 2729.
8. W. H. RHODES, *J. Am. Ceram. Soc.* **64** (1981) 19.
9. E. A. BARRINGER and H. K. BOWEN, *ibid.* **65** (1982) c-199.
10. F. F. LANGE, *ibid.* **72** (1989) 3.
11. T. IKEDA, Y. TANAKA, T. AYAKAWA and H. NOAKE, *Jpn J. Appl. Phys.* **3** (1984) 581.
12. A. I. KINGON and J. B. CLARK, *J. Am. Ceram. Soc.* **66** (1983) 253.
13. A. H. WEBSTER, T. B. WESTON and N. F. H. BRIGHT, *ibid.* **50** (1967) 490.
14. K. KAKEGAWA, J. MOHRI and S. SHIRASAKI, *ibid.* **67** (1984) c-2.
15. C. HERRING, *J. Appl. Phys.* **21** (1950) 31.
16. S. TAKAHASHI, *Jpn J. Appl. Phys.* **19** (1980) 771.
17. D. E. WITTMER and R. C. BUCHANAN, *J. Am. Ceram. Soc.* **64** (1981) 485.
18. Z. GUI, L. LI and X. ZHANG, in "Ceramic Transactions", Vol. 8, "Ceramic Dielectrics: Composition, Processing and Properties '90", edited by M. C. Ling and M. F. Yan (American Ceramic Society, Westerville, OH, 1990) pp. 82–7.
19. Z. O. ZHUANG, M. J. HAUN, S. JANG and L. E. CROSS, *Adv. Ceram. Mater.* **3** (1988) 485.
20. N. D. PATEL and P. S. NICHOLSON, *Am. Ceram. Soc. Bull.* **65** (1986) 783.
21. M. TAKAHASHI, *Jpn J. Appl. Phys.* **10** (1971) 643.
22. M. VILLEGAS, PhD thesis, Universidad Autónoma de Madrid, Spain (1993).
23. L. L. FULLMAN, *Trans. AIME* **197** (1953) 447.
24. IRE Standards on Piezoelectric Crystals: "Measurements of Piezoelectric Ceramics" (1961); *Proc. IRE* **49** (1961) 1162.
25. K. KAKEGAWA, J. MOHRI and S. SHIRASAKI, *Solid State Commun.* **24** (1977) 769.
26. J. V. BIGGERS, *Am. Ceram. Soc. Bull.* **59** (1980) 462.
27. B. V. HIREMATH, A. I. KINGON and J. V. BIGGERS, *J. Am. Ceram. Soc.* **66** (1983) 790.

28. Y. YAMAMURA, M. TANADA and H. HANEDA, *Ceram. Int.* **11** (1985) 23.
29. V. R. PALKAR and M. S. MULTANI, *Mater. Res. Bull.* **14** (1979) 1353.
30. H. L. HOLMAN and R. M. FULRATH, *J. Appl. Phys.* **44** (1973) 5227.
31. S. CHIANG, M. NISHIOKA, R. FULRATH and J. PASK, *Am. Ceram. Soc. Bull.* **60** (1981) 484.
32. K. OKAZAKI and S. NAGATA, *J. Am. Ceram. Soc.* **56** (1973) 82.
33. P. DURAN and C. MOURE, *Am. Ceram. Soc. Bull.* **64** (1985) 575.
34. R. GERSON, *J. Appl. Phys.* **31** (1960) 188.
35. R. B. ATKIN and R. M. FULRATH, *J. Am. Ceram. Soc.* **54** (1971) 113.
36. P. D. LEVETT, *Am. Ceram. Soc. Bull.* **42** (1963) 348.
37. X. L. ZHANG, Z. X. CHEN, L. E. CROSS and W. A. SCHULZE, *J. Mater. Sci.* **18** (1983) 968.
38. J. F. FERNANDEZ and C. MOURE, *Bol. Soc. Esp. Ceram. Vidr.* **27** (1988) 37.

Received 2 February
and accepted 16 February 1994